Available online at www.sciencedirect.com
ScienceDirect
Journal of Power Sources 174 (2007) 1001–1006
JOURNAL OF POWER SOURCES
www.elsevier.com/locate/jpowsour

Short communication

Theoretical examination of reference electrodes for lithium-ion cells

Dennis W. Dees *, Andrew N. Jansen, Daniel P. Abraham

Argonne National Laboratory, Argonne, IL 60439-4837, USA

Available online 28 June 2007

Abstract

An electrochemical model was developed to compare the use of internal and external reference electrodes for the study of lithium-ion cells. The impact of reference electrode placement on electrode measurements was examined using idealized reference electrodes in cells undergoing short-duration pulse currents. The effectiveness of internal reference electrodes with finite size and impedance was also examined.

Keywords: Lithium; Battery; Electrochemical; Reference; Modeling

1. Introduction

Electrochemical diagnostic tools are being used to extensively study the lithium-ion battery technology for hybrid electric vehicle applications under the Department of Energy's Advanced Technology Development (ATD) Program [1]. The majority of the electrochemical reference electrode diagnostic studies conducted under the ATD Program at Argonne National Laboratory are based on the use of a 25 μm diameter tinned copper wire that is sandwiched in a planar cell between the electrodes with at least one extra separator layer [2]. The tin layer is lithiated *in situ* to generate the reference electrode. While this is certainly one of the smallest reference electrodes used to examine any lithium-ion technology, it has several properties that make it less than optimal. The small size makes it difficult to use; conversely, the diameter of the wire is the same as a typical layer of separator. Placing the reference electrode inside the cell impacts the cell's current distribution near the reference electrode and thus may also affect the voltage measurement. An alternative to the internal reference electrode wire is using a piece of lithium placed outside the cell in a pool of electrolyte connected to the cell. This method is much easier to use and does not require the same level of miniaturization. Both the internal and external reference electrodes, when used in the same cell, often give similar, but not identical, results. The present theoretical study seeks to quantify the advantages and disadvantages of internal and external reference electrodes for lithium-ion cells.

For convenience a specific lithium-ion battery technology, used extensively in the ATD Program [2], is examined. The positive electrode (35 μm coating thickness) has a composite structure made of a layered nickel oxide ($LiNi_{0.8}Co_{0.15}Al_{0.05}O_2$) active material, a carbon black and graphite additive for distributing current, and a PVDF binder all on an aluminum current collector. The electrolyte is 1.2 M $LiPF_6$ dissolved in a mixture of EC and EMC and a Celgard microporous membrane (25 μm thickness) is used as the separator. The negative electrode (35 μm coating thickness) has a composite coating of graphite and PVDF binder all on a copper current collector. This technology is representative of a number of lithium-ion cell chemistries and considerable data is available on planar reference electrode test cells.

As an example, a special planar test cell was built with both internal and external reference electrodes. The internal reference electrode was similar to earlier studies except that four separator layers were used rather than two. A notch was cut out of the middle two layers for the 25 μm diameter tinned copper reference electrode wire. This allowed the positive and negative electrodes to lay completely flat without being pinched around the reference electrode wire. The external reference electrode was a small piece of lithium in a separator bag attached to a wire. A hybrid pulsed power characterization (HPPC) test [3] was conducted on the cell. In HPPC tests, cell voltage changes are monitored while short-duration (<20 s) high-current discharge and charge pulses are applied to the cell at various states of charge. The area specific impedance (ASI) is defined as the change in voltage during the current pulse divided by the current density of the pulse. The discharge ASI from a 10 s current pulse for the positive and negative electrodes versus cell discharge capacity

* Corresponding author.
E-mail address: dees@cmt.anl.gov (D.W. Dees).

0378-7753/$ – see front matter © 2007 Elsevier B.V. All rights reserved.
doi:10.1016/j.jpowsour.2007.06.128

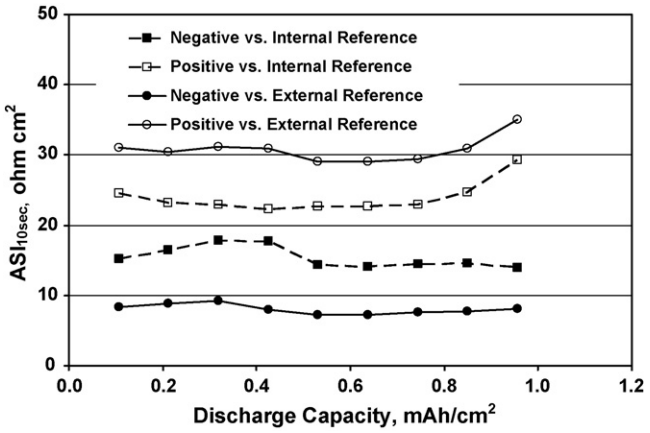

Fig. 1. Electrode area specific impedance from a 10 s discharge current pulse at 60% SOC of a lithium-ion cell with four separator layers and both internal and external reference electrodes.

for internal and external reference electrodes is given in Fig. 1. Clearly the internal reference electrode results indicate that both electrodes have similar impedance while the external reference electrode data suggests that the positive electrode has a much higher impedance than the negative.

2. Model description and development

An electrochemical model was developed for lithium-ion cells capable of comparing the attributes of internal and external reference electrodes. The general methodology for the electrochemical model follows the work of Professor Newman at Berkeley [4] and is similar to several other electrochemical models presented over the last 15 years [5–9]. The model development in the present study is the same as used in earlier work [10] except that a more simplified approach is utilized to account for interfacial effects. Concentrated solution theory is used to describe the salt transport through the electrolyte and volume-averaged transport equations account for the porous separator and composite electrode structure. The electrolyte transport equations in this study, given by Eqs. (1)–(3) below (see Table 1 for the nomenclature) is based on the volume-averaged velocity of the electrolyte. Also below are the remaining current expressions (Eqs. (4) and (5)) needed for the cells overall current balance, and the transport expression for the lithium diffusion in the active materials (Eq. (6)).

$$\varepsilon\frac{\partial c}{\partial t} = \frac{\varepsilon}{\tau}\nabla\cdot(D\nabla c) + \frac{\nabla\cdot\left[\left(1-c\bar{V}_e\right)\left(1-t_+^0\right)\vec{i}_2\right]}{z_+\nu_+F} \tag{1}$$

$$\vec{i}_2 = -\frac{\kappa\varepsilon}{\tau}\nabla\Phi_2 - \nu RT\frac{\kappa\varepsilon}{F\tau}\left(\frac{s_+}{n\nu_+} + \frac{t^0}{z_+\nu_+}\right) \times\left(1+\frac{\partial\ln f_\pm}{\partial\ln c}\right)\nabla\ln c \tag{2}$$

$$\nabla\cdot\vec{i}_2 = Fz_+aj_n \tag{3}$$

$$\vec{I} = \vec{i}_1 + \vec{i}_2 \tag{4}$$

$$\vec{i}_1 = -\sigma_{\text{eff}}\nabla\Phi_1 \tag{5}$$

Table 1
Equation nomenclature

Symbol	Description
a	Specific interfacial area
c	Electrolyte salt concentration
c_{ref}	Reference electrolyte salt concentration
c_S	Lithium concentration in active material
$c_{S,\text{ref}}$	Reference lithium concentration in active material
c_T	Maximum lithium concentration in active material
D	Salt diffusion coefficient in electrolyte
D_s	Lithium diffusion coefficient in active material
$f_\pm$	Electrolyte salt activity coefficient
F	Faraday's constant
i_1	Superficial electronic current density
i_2	Superficial ionic current density
i_0	Kinetic exchange current density
i_n	Transfer current per unit of interfacial area
I	Superficial total cell current density
j_n	Pore-wall flux density
n	Electrons transferred in electrochemical reaction
R	Universal gas constant
s_+	Cation stoichiometric coefficient
t	Time
t_+^0	Cation transference number
T	Temperature
U	Oxide open circuit potential
$\bar{V}_e$	Partial molar volume of the electrolyte
z_+	Cation charge number
α_A, α_C	Transfer coefficients
σ_{SEI}	SEI area specific resistance
σ_{eff}	Effective electrode electronic conductivity
ε	Volume fraction of electrolyte
τ	Electrolyte tortuosity
υ_+	Cations per salt molecule
υ	Ions per salt molecule
η_{SEI}	SEI resistance potential loss
Φ_1	Potential of electronically conducting matrix
Φ_2	Electrolyte potential

$$\frac{\partial c_S}{\partial t} = \nabla\cdot(D_S\nabla c_S) \tag{6}$$

As described in earlier work [10] the electrolyte-active material interface in lithium-ion electrodes, often referred to as the solid electrolyte interface or SEI, is ill defined and very complicated. The process of moving lithium-ions across the SEI includes some combination of diffusion, migration, and reaction. While it is critically important to account for the potential effects associated with the SEI it is beyond the scope of this study to include a detailed description of the SEI in the model. There are a number of alternatives given below, which can be utilized. The Butler–Volmer reaction expression given by Eq. (7) is the most widely accepted equation to describe the kinetics for an electrochemical reaction. However, the interfacial overpotential for the present technology is a relatively linear function of current density. This can be seen from the electrode's ASI for a 1 s discharge pulse as a function of pulse current density given in Fig. 2.

Most if not all of the electrode's interfacial effects reach steady-state in 1 s and the ASI measurements are relatively independent of current density over a wide range. Alternatively, a linear overpotential function (see Eq. (8)) or a combined

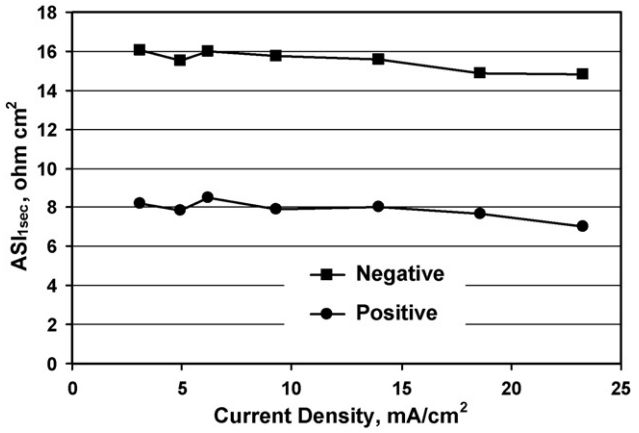

Fig. 2. Electrode area specific impedance from a 1 s discharge current pulse of a lithium-ion reference cell with two separator layers at 60% SOC.

Butler–Volmer and linear overpotential function (see Eq. (9)) can be used [7]. Another option, a linear Butler–Volmer kinetic expression given by Eq. (10), is utilized in the present study. This expression helps simplify and stabilize the calculations, as well as accounting for some of the observed increase in positive interfacial ASI at low states-of-charge (SOC). For the present system at 60% SOC and pulse current densities less than around 5 mA cm^{-2}, all of these expressions are essentially equivalent. The conclusions drawn from the present study are expected to be independent of the interfacial expression utilized.

$$i_n = i_0\left(\frac{c}{c_{\text{ref}}}\right)^{\alpha_A}\left(\frac{c_T - c_S}{c_T - c_{S,\text{ref}}}\right)^{\alpha_A}\left(\frac{c_S}{c_{S,\text{ref}}}\right)^{\alpha_C} \times \left\{\exp\left[\frac{\alpha_A F}{RT}(\Phi_1 - \Phi_2 - U)\right] - \exp\left[-\frac{\alpha_C F}{RT}(\Phi_1 - \Phi_2 - U)\right]\right\} \quad (7)$$

$$\eta_{\text{SEI}} = \sigma_{\text{SEI}} i_n = \sigma_{\text{SEI}} z_+ F j_n \quad (8)$$

$$i_n = i_0\left(\frac{c}{c_{\text{ref}}}\right)^{\alpha_A}\left(\frac{c_T - c_S}{c_T - c_{S,\text{ref}}}\right)^{\alpha_A}\left(\frac{c_S}{c_{S,\text{ref}}}\right)^{\alpha_C} \times \left\{\begin{array}{l}\exp\left[\frac{\alpha_A F}{RT}(\Phi_1 - \Phi_2 - U - \eta_{\text{SEI}})\right] - \\ \exp\left[-\frac{\alpha_C F}{RT}(\Phi_1 - \Phi_2 - U - \eta_{\text{SEI}})\right]\end{array}\right\} \quad (9)$$

$$i_n = i_0\left(\frac{c}{c_{\text{ref}}}\right)^{\alpha_A}\left(\frac{c_T - c_S}{c_T - c_{S,\text{ref}}}\right)^{\alpha_A}\left(\frac{c_S}{c_{S,\text{ref}}}\right)^{\alpha_C} \times \left[\frac{(\alpha_A + \alpha_C)F}{RT}(\Phi_1 - \Phi_2 - U)\right] \quad (10)$$

The system of coupled time-dependent non-linear multi-dimensional partial differential equations (Eqs. (1)–(6), and (10)) was solved using a partial differential equation solver (FlexPDE). The geometries considered in this study are all two-dimensional with the diffusion of lithium in the electrode active material particles adding a pseudo third dimension. As described in a previous study [11], the active material particles were radially discretized using a finite difference form of the differential diffusion equation (Eq. (6)). The lithium concentration at the individual nodes of the active material particles was then carried as dependent variables in the numerical two-dimensional solver. To insure an accurate mass balance of lithium in the active material particles, the actual, rather than the approximate, volume element was used in the finite difference form of the differential diffusion equation. The general approach to the parameter estimation is described elsewhere [10]. In this study, the electrolyte transport and thermodynamic parameters were estimated using the advanced electrolyte model of Gering [12], which agreed well with experimental measurements [13].

3. Results and discussion

As a first step to examining the internal and external reference electrodes, a series of simulations of a lithium-ion cell with an edge, shown in Fig. 3, undergoing a 10 s HPPC discharge pulse where conducted. The internal reference electrode is placed on the left hand side of the cell in the middle of the separator layers. The cell length is taken to be long enough that potential lines near the internal reference electrode are uniform. There is a pool of electrolyte outside the cell edge where the external reference electrode is placed close to the upper right hand corner. This geometry is similar to the cell edge of the 32 cm^2 area lab cell fixtures extensively used in the ATD studies [2] and the results presented can be extended to other cell geometries such as pouch cells and Swagelok T-cells with similar conclusions. It is assumed in this modeling study that the internal and external reference electrodes are ideal (i.e. have infinitesimal size and are reversible). Optimally one would want to measure the potential in the electrolyte next to the electrode of interest, but since both electrodes are potentially of interest placing the reference electrode midway between the positive and negative electrodes in a region of uniform current distribution would be the best compromise. Since this description coincides with the internal reference electrode's placement, the external reference will be compared to the internal results.

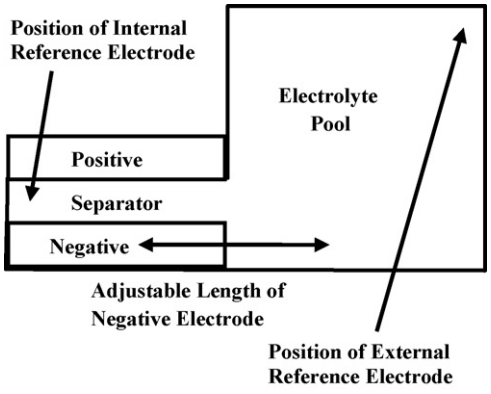

Fig. 3. Diagram of lithium-ion cell edge showing position of internal and external reference electrodes.

Fig. 4. Simulation of electrolyte potential distribution near edge of a lithium-ion cell (see Fig. 3) with electrodes aligned at 10 s into a 5 C discharge pulse at 60% SOC. Lettered isopotential lines are shown at about 4 mV intervals.

The potential distribution in the electrolyte, near the edge of the cell, at the end of a 5 mA cm^{-2} 10 s discharge pulse at 60% SOC is shown in Fig. 4 for a cell with the positive and negative electrodes perfectly aligned. A close examination of the isopotential lines shows that there is very little potential change in the pool of electrolyte away from the edge of the cell. Further, the potential of the electrolyte in the pool is essentially the same as that of the center of the cell. Thus the internal and external reference electrodes would yield essentially the same result. However, if the positive and negative electrodes are misaligned, even by a fraction of a millimeter, the results are dramatically different, as shown in Figs. 5 and 6. In these figures the isopotential lines are severely distorted near the edge even with only a 0.4 mm misalignment. Depending on which electrode overlaps the other the potential of the electrolyte pool is essentially that of the electrolyte in one of the electrodes near the edge.

The variation in positive electrode ASI based on an external reference electrode and internal reference electrode potential with the extent of misalignment is given in Fig. 7. In the figure, one can see that the ASI of the positive electrode is relatively

Fig. 5. Simulation of electrolyte potential distribution near edge of a lithium-ion cell (see Fig. 3) with negative electrode extending 0.4 mm past the positive at 10 s into a 5 C discharge pulse at 60% SOC. Lettered isopotential lines are shown at about 5 mV intervals.

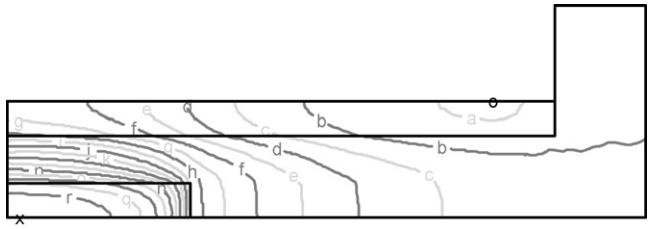

Fig. 6. Simulation of electrolyte potential distribution near edge of a lithium-ion cell (see Fig. 3) with positive electrode extending 0.4 mm past the negative at 10 s into a 5 C discharge pulse at 60% SOC. Lettered isopotential lines are shown at about 5 mV intervals.

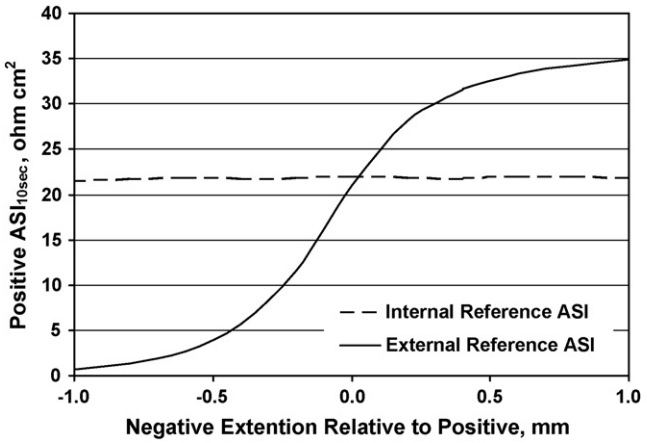

Fig. 7. Simulation of positive area specific impedance of a lithium-ion cell with four separator layers at 10 s into a 5 C discharge pulse at 60% SOC as a function of negative electrode misalignment.

constant when measured with the internal reference electrode, but varies significantly when using the external. While it is difficult to align the electrodes to within a millimeter, the variation in the external reference electrode begins to level off at about the 0.4 mm misalignment. Unfortunately, the errors introduced are quite significant. Because the overall cell impedance does not depend on the reference electrode, errors in one electrode measurement are reflected in the opposite direction for the other electrode as shown in Fig. 8 for the negative electrode.

Fortunately, other than electrode alignment, the difference in electrode ASI measured with internal and external reference electrodes tends not to be a strong function of cell design or operating conditions. While examining all aspects of cell design and operating conditions is beyond the scope of this paper, two examples that were studied include the variation in positive electrode ASI with pulse current density and separator thickness as given in Figs. 9 and 10, respectively. In both of these examples the use of either the internal or external reference electrode results in the same change in positive electrode ASI. Similarities in the variation of electrode ASI is what really makes the

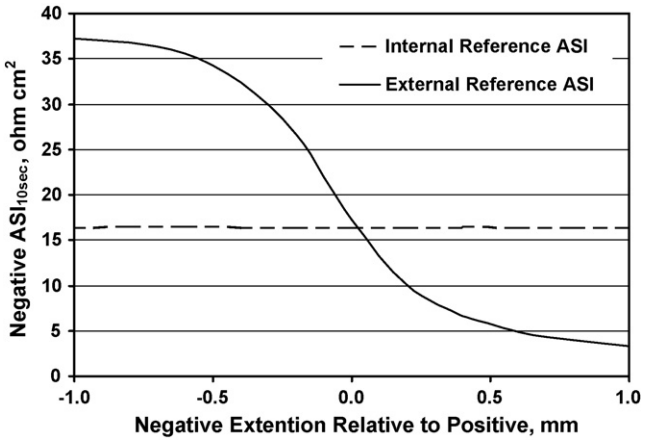

Fig. 8. Simulation of negative area specific impedance of a lithium-ion cell with four separator layers at 10 s into a 5 C discharge pulse at 60% SOC as a function of negative electrode misalignment.

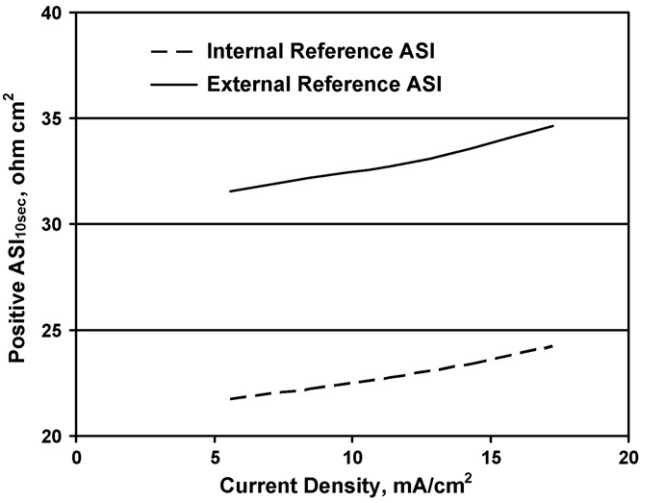

Fig. 9. Simulation of positive area specific impedance of a lithium-ion cell with four separator layers and a 0.4 mm negative electrode extension at 10 s into a discharge pulse at 60% SOC as a function of discharge current density (5 mA cm^{-2} is a 5 C pulse).

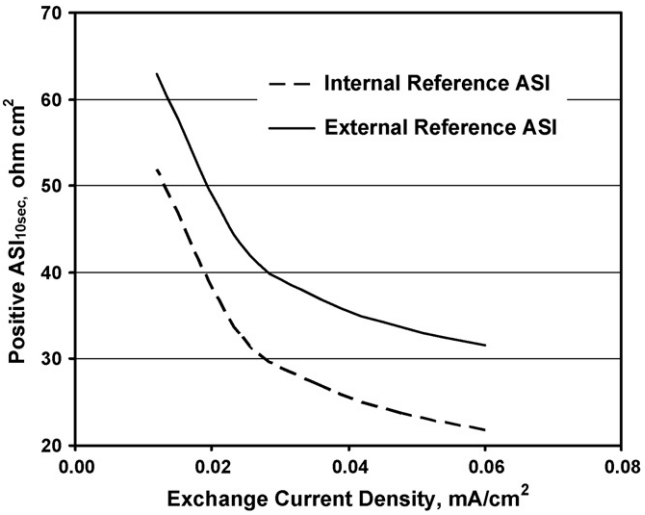

Fig. 11. Simulation of negative area specific impedance of a lithium-ion cell with four separator layers and a 0.4 mm negative electrode extension at 10 s into a 5 C discharge pulse at 60% SOC as a function of exchange current density (i_0).

external reference electrode a viable tool to examine electrode performance of lithium-ion cells as shown in Fig. 11, which gives the change in ASI with exchange current density. In the model the exchange current density is inversely proportional to the interfacial impedance and Fig. 11 shows that both the internal and external reference electrodes are equally capable of tracking absolute changes in electrode impedance.

A limited number of simulations were conducted on an internal reference electrode of a finite size for the 25 μm diameter reference electrode wire used in the ATD Program (see Fig. 12). A linear overpotential expression is assumed on the surface of the reference electrode (see Eq. (8)). The presence of the reference electrode distorts the electrolyte's current, concentration, and potential distribution in its vicinity. As an example, the electrolyte potential distribution in the vicinity of the reference electrode wire is shown in Fig. 13.

The distortion of the electrolyte potential distribution in the vicinity of the wire is obviously not desirable. However, for the 25 μm diameter reference electrode wire the variation in potential from the ideal value, as defined by the electrolyte potential at the midpoint of the separator far from the wire, tends to be less than a millivolt. Of potentially more concern is the electrolyte current that travels through the reference electrode rather than going around it. When current is passed through the cell, a small fraction of the current goes into the reference electrode via a reduction or oxidation reaction on one side and comes out the other through the counter electrochemical reaction. As the amount of charge passed through the reference electrode approaches its capacity, the reference electrode would start to polarize. The typical experimentally measured capacity loaded into the 25 μm diameter reference electrode wire is ~0.1 μAh cm^{-1} of exposed wire. Simulations indicate that for a 5 mA cm^{-2} cell current about 35 μA cm^{-2} pass through the

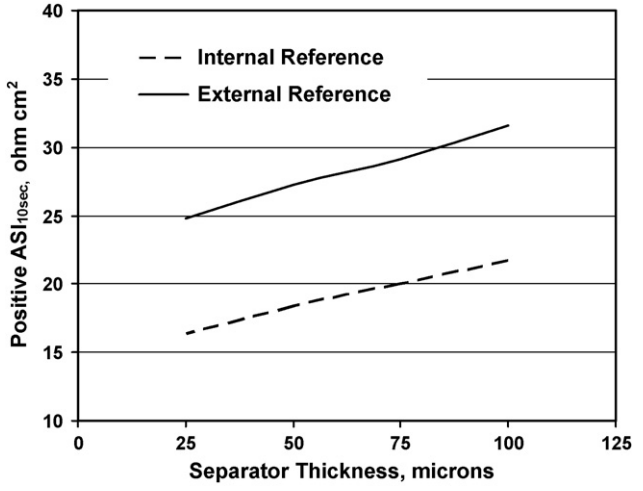

Fig. 10. Simulation of positive area specific impedance of a lithium-ion cell with a 0.4 mm negative electrode extension at 10 s into a 5 C discharge pulse at 60% SOC as a function of separator thickness (a separator layer is 25 μm thick).

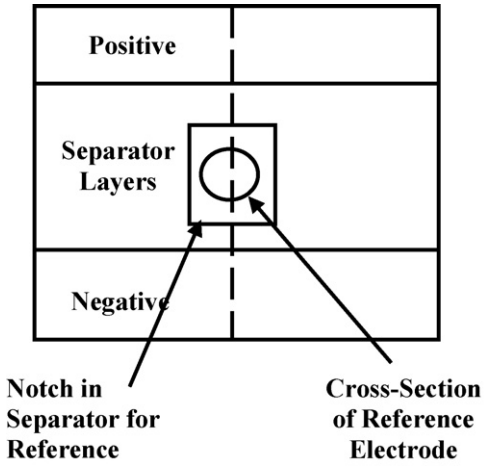

Fig. 12. Cross-sectional diagram of lithium-ion cell with four separator layers showing position of 25 μm internal reference electrode wire. Line of symmetry used in simulations shown by dashed line.

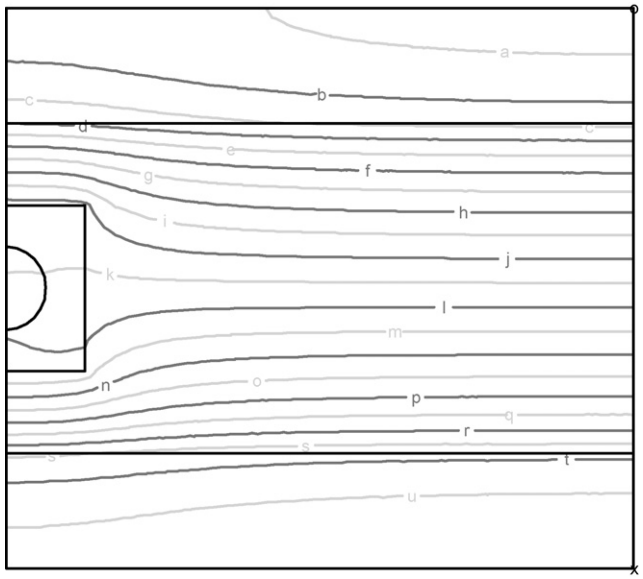

Fig. 13. Simulation of electrolyte potential distribution of a lithium-ion cell (see Fig. 12) at 10 s into a 5 C discharge pulse at 60% SOC. Lettered isopotential lines are shown at about 5 mV intervals.

wire (based on a 100 Ω cm^2 interfacial reaction impedance for the wire). The charge passed during a 10 s discharge pulse would be about three orders-of-magnitude lower than the reference electrode wire capacity.

As one would expect, as the size of the reference electrode grows its impact on the cell and the electrode measurements becomes significant. Simulations indicate that the potential of a 25 μm thick, 1 mm wide reference electrode strip in a lithium-ion cell would vary from the ideal value by more than 10 mV during a 5 C discharge pulse.

4. Conclusions

Reference electrode size and placement, along with cell geometry, has a significant effect on the measured electrode impedance in lithium-ion cells. Observable differences between electrode measurements using both internal and external reference electrodes can be explained from edge effects connected with positive and negative electrode alignment during cell assembly and their interaction with the external reference electrode.

A 25 μm diameter internal reference electrode wire placed between separator layers distorts the potential and concentration profiles in the surrounding electrolyte, but does not significantly impact the accuracy of the impedance measurement. Therefore, it is an effective technique to examine electrode potentials in lithium-ion cells. Depending on its shape and size, larger internal reference electrodes can impact the electrode impedance measurement. Even a 25 μm thick, 1 mm wide reference electrode has a measurable impact (i.e. ∼10% error) on the electrode impedance in lithium-ion cells.

External reference electrodes are easier to implement, but generate errors depending on positive electrode and negative electrode alignment. These errors actually approach the size of the impedance measurement for electrodes misaligned by as little as 1 mm. The sensitivity of these reference electrodes to cell assembly effectively makes them not useful for measuring the absolute value of the electrode impedance. Fortunately, these errors are generally fixed, making the external reference electrode a useful tool for following changes in electrode impedance.

The similarities between the present lithium-ion cell and most other lithium-ion technologies suggest that the conclusions drawn here are relatively general. They should also be applicable to other cell geometries, such as pouch cells and Swagelok T-cells. The relative impact of a specific internal reference electrode geometry and its electrochemical characteristics would have to be examined on a case-by-case basis. However as a guide, reference electrodes with characteristic lengths less than or on the order of the separator thickness would be acceptable.

Acknowledgements

The authors thank Tien Duong and David Howell of the FreedomCAR and Vehicle Technologies Program at the U.S. Department of Energy, Office of Energy Efficiency and Renewable Energy for their support.

The submitted manuscript has been created by the University of Chicago as Operator of Argonne National Laboratory (“Argonne”) under Contract No. W-31-109-ENG-38 with the U.S. Department of Energy. The U.S. Government retains for itself, and others acting on its behalf, a paid-up, non-exclusive, irrevocable worldwide license in said article to reproduce, prepare derivative works, distribute copies to the public, and perform publicly and display publicly, by or on behalf of the Government.

References

[1] D. Howell, Energy Storage Research and Development, 2005 Annual Progress Report, FreedomCAR and Vehicle Technologies Program, Energy Efficiency and Renewable Energy, January 2006.
[2] D.P. Abraham, S.D. Poppen, A.N. Jansen, J. Liu, D.W. Dees, Electrochim. Acta 49 (2004) 4763.
[3] PNGV Battery Test Manual, DOE/ID-10597, Rev. 3.(2001).
[4] J. Newman, K. Thomas-Alyea, Electrochemical Systems, John Wiley and Sons, New York, 2004.
[5] M. Doyle, T. Fuller, J. Newman, J. Electrochem. Soc. 140 (1993) 1526.
[6] T. Fuller, M. Doyle, J. Newman, J. Electrochem. Soc. 141 (1994) 1.
[7] M. Doyle, J. Newman, J. Electrochem. Soc. 143 (1996) 1890.
[8] R. Darling, J. Newman, J. Electrochem. Soc. 144 (1997) 4201.
[9] V. Srinivasan, J. Newman, J. Electrochem. Soc. 151 (2004) A1530.
[10] D. Dees, E. Gunen, D. Abraham, A. Jansen, J. Prakash, J. Electrochem. Soc. 152 (2005) A1409.
[11] D. Dees, V. Battaglia, A. Belanger, J. Power Sources 110 (2002) 310.
[12] K.L. Gering, T.Q. Duong, Prediction of Electrolyte Transport Properties Using a Solvation based Chemical Physics Model, in: Proceedings of the Electrochemical Society 204th Meeting, Orlando, FL, October 12–16, 2003.
[13] E. Gúnen, Dissertation, Illinois Institute of Technology, Chicago, IL, 2003.